

Determination of the \bar{K}^0d scattering length from the reaction $pp \rightarrow d\bar{K}^0K^+$

A. Sibirtsev^a, M. Büscher^a, V.Yu. Grishina^b, C. Hanhart^a, L.A. Kondratyuk^c, S. Krewald^a,
U.-G. Meißner^{a d}

^aInstitut für Kernphysik, Forschungszentrum Jülich, D-52425 Jülich, Germany

^bInstitute for Nuclear Research, 60th October Anniversary Prospect 7A, 117312 Moscow, Russia

^cInstitute of Theoretical and Experimental Physics, B. Chermushkinskaya 25, 117218 Moscow, Russia

^dUniversität Bonn, Helmholtz-Institut für Strahlen und Kernphysik (Theorie), Nußallee 14-16, D-53115 Bonn, Germany

The real and imaginary parts of the \bar{K}^0d scattering length are extracted from the \bar{K}^0d mass spectrum obtained from the reaction $pp \rightarrow d\bar{K}^0K^+$ measured recently at the Cooler Synchrotron COSY at Jülich. We extract a new limit on the K^-d scattering length, namely $\text{Im } a \leq 1.3$ fm and $|\text{Re } a| \leq 1.3$ fm. The limit for the imaginary part of the K^-d scattering length is supported by data on the total K^-d cross sections.

During the last two decades the physics of the low-energy $\bar{K}N$ and $\bar{K}A$ interactions has gained substantial interest. A well-known K -matrix analysis [1] of the available K^-N data led to the conclusion that the real part of the s -wave K^-p scattering length is repulsive, $\text{Re } a_{K^-p} = -0.7$ fm, while the real part of the K^-n scattering length is attractive, $\text{Re } a_{K^-n} = 0.37$ fm. In a recent KEK experiment the strong interaction shift of the kaonic hydrogen atom $1s$ state was found to be repulsive [2], corresponding to a negative K^-p scattering length. The first results for kaonic hydrogen from the DEAR experiment also indicate a repulsive shift [3]. However, at the same time there are no direct experimental results available for the K^-n scattering length. From a theoretical point of view it is natural to expect that the K^-N interaction, averaged over proton and neutron targets, is attractive. One of the fundamental reasons for this expectation is given by the leading order term in the chiral expansion for the K^-N channel which appears to be attractive (in contrast to the isoscalar pion-nucleon scattering amplitude). In fact it is possible to have a negative scattering length $\text{Re } a_{K^-p}$ for the attractive $\bar{K}N$ interaction if the $\Lambda(1405)$ resonance is

a bound state of $\bar{K}N$ system [4,5]. Such a peculiar dynamics of the elementary $\bar{K}N$ interaction implies non-trivial properties of anti-kaons in finite nuclei and dense nuclear matter, including neutron stars, see e.g. Refs. [6,7,8,9] (and references therein). A renewed interest in physics with low-energy kaons was initiated by substantial progress in effective low energy hadronic methods, in particular by approaches based on extensions of chiral perturbation theory, for early reviews see Refs. [10,11,12,13]. The coupled channel dynamics of the $\bar{K}N$ interaction based on tree level chiral Lagrangians was developed in order to describe low-energy scattering data [14,15,16] and giving further support to the description of the $\Lambda(1405)$ as a meson-baryon bound state (a new twist on this story was given in Ref. [17], where the two-pole structure of this state was investigated). However, it was shown recently [18] that a reliable extraction of the elementary $\bar{K}N$ scattering length from such type of approach requires an explicit matching of the amplitudes generated from the coupled channel dynamics to the ones given from chiral perturbation theory [19]. This matching can even be done in some unphysical region of the corresponding Mandelstam plane. If

this is not done, the calculations result in very large K^-p and K^-n scattering lengths, which contradict the experimental results [1] and might stem from the implicit violation of chiral symmetry. Therefore, new and more exact experimental results on K^-p and K^-n scattering are necessary in order to obtain reliable constraints on the K^-N dynamics and to gain a better understanding of the description of SU(3) chiral symmetry breaking. The measurement of the K^-d scattering length is one of the main goals of the SIDHARTA experiment at DAΦNE [20]. In [18] the precise relation between the energy-shift in kaonic hydrogen and the appropriate scattering lengths combination is worked out.

In this paper we show that constraints on the $\bar{K}d$ scattering length can be obtained through an analysis of the \bar{K}^0d final-state interaction (FSI) in the reaction $pp \rightarrow d\bar{K}^0K^+$ near threshold measured very recently at COSY [21]. Theoretical analyses of the reaction $pp \rightarrow \bar{K}^0dK^+$ near threshold have been performed in Refs.[22,23,24,25,26,27]. As has been stressed in Ref. [23], the $NN \rightarrow d\bar{K}K$ reaction should be sensitive to the $\bar{K}d$ FSI. Thus one can expect that the experimental results on the $pp \rightarrow d\bar{K}^0K^+$ reaction may provide a new way to extract the \bar{K}^0d scattering length.

In this paper we focus on the potential influence of the $\bar{K}d$ interaction on the observables for the process $pp \rightarrow d\bar{K}^0K^+$. The effect of the $\bar{K}K$ s -wave interaction can be investigated via the inclusion of a Flatté distribution for the $a_0(980)$. This had a negligible effect on the shape spectra [21]. A study of a possible interplay of the $\bar{K}d$ and the $\bar{K}K$ interaction will be presented in a subsequent publication. However, the data is compatible with a quite weak $\bar{K}d$ interaction only and therefore adding the $\bar{K}K$ interaction is not expected to change the picture significantly.

Near threshold the partial wave structure of the final-state for the $pp \rightarrow d\bar{K}^0K^+$ reaction can be described by the superposition of two configurations $[(\bar{K}^0K^+)_s d]_P$ and $[(\bar{K}^0K^+)_p d]_S$ with the \bar{K}^0K^+ -system in the s - and p -wave, respectively. Correspondingly, the deuteron is in a p -wave (or s -wave) with respect to the \bar{K}^0K^+ -system in the first (or second) case. An overall s -wave is for-

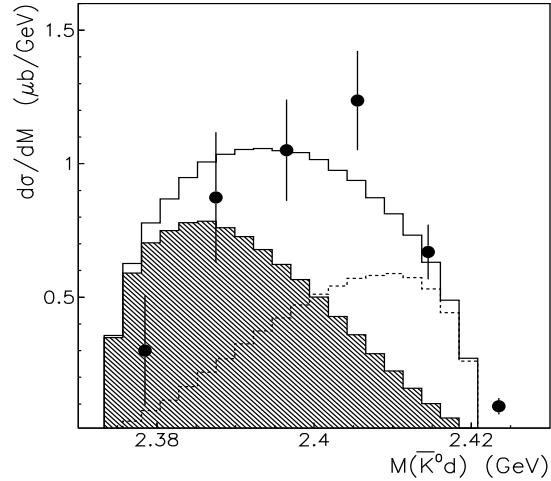


Figure 1. \bar{K}^0d mass spectra from the reaction $pp \rightarrow d\bar{K}^0K^+$ at $T_p=2.65$ GeV, i.e. an excess energy of 46 MeV. The experimental results are taken from Ref. [21]. The experimental mass resolution is $\simeq 3$ MeV. The hatched histogram indicates the \bar{K}^0d s -wave contribution, dashed- p -wave and solid is their sum.

bidden by selection rules.

Therefore, if we restrict ourselves to these partial waves, the most general spin-averaged squared matrix element is given as

$$\begin{aligned} |\overline{M(\mathbf{q}, \mathbf{k})}|^2 = & C_0^q q^2 + C_0^k k^2 + C_1 (\hat{\mathbf{p}} \cdot \mathbf{k})^2 \\ & + C_2 (\hat{\mathbf{p}} \cdot \mathbf{q})^2 + C_3 (\mathbf{k} \cdot \mathbf{q}) + C_4 (\hat{\mathbf{p}} \cdot \mathbf{k})(\hat{\mathbf{p}} \cdot \mathbf{q}) \end{aligned} \quad (1)$$

where $\hat{\mathbf{p}} = \mathbf{p}/|\mathbf{p}|$ and \mathbf{p} is the initial center-of-mass (c.m.) momentum, \mathbf{k} is the final c.m. momentum of the deuteron, and \mathbf{q} is the relative c.m. momentum of the \bar{K}^0K^+ -system. Furthermore, the six real coefficients C_i can be expressed through the corresponding partial wave amplitudes [24,25].

In Ref. [21] the parameters C_i were extracted from the data at a proton beam energy of $T_p=2.65$ GeV. The parameters C_0^q and C_2 account for the contributions from the $\bar{K}\bar{K}$ p -wave, C_0^k and C_1 from the $\bar{K}\bar{K}$ s -wave and C_3 and C_4 stem from s - p interference.

To analyze the \bar{K}^0d FSI in the s -wave it is necessary to isolate the \bar{K}^0d s -wave contribution from the $pp \rightarrow d\bar{K}^0K^+$ reaction. Therefore we should express the matrix element in terms of

the partial amplitudes in a basis that is different to the one given above, namely in terms of $[(\bar{K}^0 d)_s K^+]_P$ and $[(\bar{K}^0 d)_p K^+]_S$ states, where the $\bar{K}^0 d$ -system is in the s - and p -wave, respectively. As was proposed in Ref. [26] the vectors of Eq. (1) can be expressed in terms of the c.m. momentum of the K^+ , \mathbf{P} , and the relative momentum of the $\bar{K}^0 d$ system, \mathbf{Q} , as

$$\mathbf{q} = \mathbf{Q} - \alpha \mathbf{P}, \quad \mathbf{k} = \frac{1}{2}((2 - \alpha)\mathbf{P} + \mathbf{Q}), \quad (2)$$

where $\alpha = m_d / (m_d + m_{\bar{K}})$. The squared amplitude expressed in the new frame reveals the same structure as Eq. (1), namely:

$$\begin{aligned} |M(\mathbf{Q}, \mathbf{P})|^2 = & B_0^Q Q^2 + B_0^P P^2 + B_1(\mathbf{P} \cdot \hat{\mathbf{p}})^2 \\ & + B_2(\mathbf{Q} \cdot \hat{\mathbf{p}})^2 + B_3(\mathbf{P} \cdot \mathbf{Q}) + B_4(\mathbf{P} \cdot \hat{\mathbf{p}})(\mathbf{Q} \cdot \hat{\mathbf{p}}), \end{aligned} \quad (3)$$

where the B_i coefficients can be expressed in terms of the C_i from Eq. (1) and

$$\begin{aligned} B_0^P = & \frac{(2 - \alpha)^2}{4} C_0^k + \alpha^2 C_0^q - \frac{\alpha(2 - \alpha)}{2} \frac{1}{2} C_3, \\ B_1 = & \frac{(2 - \alpha)^2}{4} C_1^k + \alpha^2 C_1^q - \frac{\alpha(2 - \alpha)}{2} \frac{1}{2} C_4. \end{aligned} \quad (4)$$

Using the results of the fit for C_i from Ref. [21] we obtain the following values for the coefficients B_i : $B_0^Q = 0.81$, $B_0^P = 0.705$, $B_1 = -0.267$, $B_2 = -0.267$, $B_2 = -1.45$, $B_3 = 1.41$. It follows from this that the $\bar{K}^0 d$ s -wave contributes 57% to the total cross section. Fig. 1 shows the $\bar{K}^0 d$ mass spectra from the $pp \rightarrow d \bar{K}^0 K^+$ reaction at the beam energy $T_p = 2.65$ GeV [21]. The histograms show our calculations with the parameters B_i given above. The hatched histogram shows the $\bar{K}^0 d$ s -wave contribution, the dashed line illustrates the p -wave contribution, while the solid histogram shows the result of our full calculation. We recall that in Ref. [21] the parameters C_i were obtained from a joint fit to $\bar{K}^0 K^+$ and $\bar{K}^0 d$ mass spectra as well as $\cos(\mathbf{p}\mathbf{k})$, $\cos(\mathbf{p}\mathbf{q})$ and $\cos(\mathbf{k}\mathbf{q})$ angular distributions.

Since we isolate the s -wave contribution from the $\bar{K}^0 d$ mass spectrum it is now possible to study the interaction between the final \bar{K}^0 -meson and the deuteron. Following the standard Watson and Migdal theorem [32,33,34] we include the FSI by multiplying the $B_0^P P^2$ and $B_1(\hat{\mathbf{p}} \cdot \mathbf{P})^2$ terms by

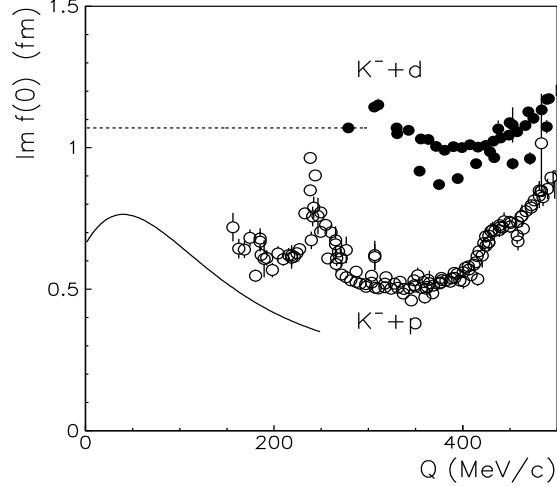


Figure 2. Imaginary part of the $K^- d$ and the $K^- p$ forward scattering amplitudes, respectively, as a function of the cms momentum Q . The data were obtained from total cross sections using the optical theorem. The solid line shows the K -matrix solution for $K^- p$ s -wave amplitude given by Martin [1]. The dashed line shows our extrapolation for $K^- d$ amplitude.

the enhancement factor $|1 - iQa|^{-2}$, where a is the complex scattering length. After that correction we refit the experimental $\bar{K}^0 d$ invariant mass distribution with two free parameters, namely the real and imaginary parts of the $\bar{K}^0 d$ scattering length, while keeping the $\bar{K}^0 d$ s -wave distribution fixed. We also checked that the influence of this additional energy dependence does not significantly change the other observables given in Ref. [21] that went into the fit of the C_i parameters.

Before performing the fit, we have to specify the boundary conditions for the $\bar{K}^0 d$ scattering length a . While there are no experimental constraints on the real part $\text{Re } a$ of the $\bar{K}^0 d$ scattering length, it is clear that $\text{Im } a$ must be positive because of unitarity. Furthermore, a lower bound on the imaginary part can be deduced from the experimental data on the $K^- d$ total cross section σ_{tot} using the optical theorem for the forward scattering amplitude

$$\text{Im } f(0) = \frac{Q \sigma_{\text{tot}}}{4\pi}, \quad a = f(0) |_{Q \rightarrow 0}. \quad (5)$$

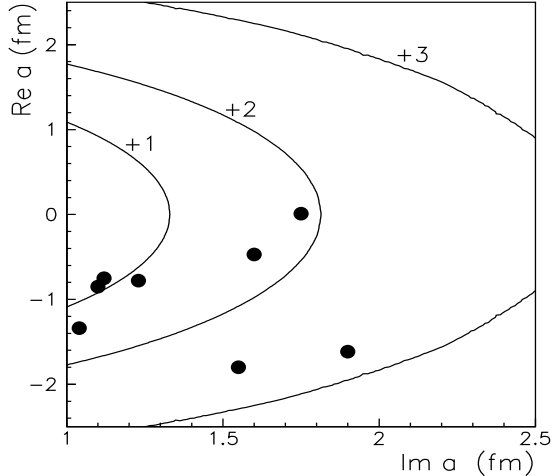


Figure 3. Real versus imaginary part of the $\bar{K}^0 d$ scattering length. The solid contour lines show the results of our fit to the $pp \rightarrow d\bar{K}^0 K^+$ data [21] for χ^2+1 , χ^2+2 and χ^2+3 . The solid circles show the results from model calculations collected in Table 1.

Fig. 2 shows the imaginary part of the $K^- d$ forward scattering amplitude as a function of the c.m. momentum Q deduced from the data on the $K^- d$ total cross section (solid circles). The extrapolation below 300 MeV/c by a straight dashed line gives $\text{Im } a \simeq 1.1$ fm. However, one might argue whether this momentum independent extrapolation can be considered as being realistic, since the contribution from the $\Lambda(1405)$ and $\Sigma(1385)$ resonances might be quite strong at small Q .

To investigate that problem we show by the open circles in Fig. 2 the imaginary part of the $K^- p$ forward scattering amplitude. The extrapolation below 200 MeV/c by the straight line gives for the imaginary part of $K^- p$ scattering length $\simeq 0.7$ fm. This bound for the imaginary part of the $K^- p$ scattering length agrees with the K -matrix solution for the $K^- p$ s -wave amplitude found by Martin [1]. Note that the K -matrix solution includes the $\Lambda(1405)$ and $\Sigma(1385)$ resonances and the momentum dependence of $f(0)$ obtained from the K -matrix is shown by the solid line in Fig. 2. Obviously the K -matrix result underestimates the data on the imaginary part of the $K^- p$

Table 1

The $K^- d$ scattering lengths predicted by different calculations with various elementary $K^- p$ and $K^- n$ scattering lengths. Here, FCA denotes the fixed center approximation, while FE stands for the calculations by Faddeev equations. All values are in fm.

$a(K^- N)$	$K^- d$	Ref.
$K^- p = -0.66 + i0.67$ $K^- n = 0.264 + i0.57$	FCA $-0.78 + i1.23$	[27]
$K^- p = -0.70 + i0.71$ $K^- n = 0.28 + i0.67$	FE $-1.34 + i1.04$	[28]
$K^- p = -0.66 + i0.67$ $K^- n = 0.26 + i0.57$	FCA $-0.75 + i1.12$	[29]
$K^- p = -0.66 + i0.67$ $K^- n = 0.26 + i0.57$	FE $-0.85 + i1.10$	[29]
$K^- p = -0.045 + i0.835$ $K^- n = 0.94 + i0.72$	FCA $-0.01 + i1.75$	[29]
$K^- p = -0.045 + i0.835$ $K^- n = 0.94 + i0.72$	FE $-0.47 + i1.60$	[29]
$K^- p = -0.789 + i0.929$ $K^- n = 0.574 + i0.619$	FCA $-1.615 + i1.909$	[30]
$K^- p = -1.01 + i0.95$ $K^- n = 0.54 + i0.53$	FE $-1.92 + i1.58$	[31]

forward scattering amplitude at $Q \geq 160$ MeV/c, since this solution does not include all channels that are open at high momenta. Based on these arguments we finally conclude that a reasonable estimate of the lower limit for the imaginary part of $\bar{K}^0 d$ scattering length is about 1 fm. Therefore, we fit the experimental results [21] for the $\bar{K}^0 d$ invariant mass spectrum using the lower bound $\text{Im } a \geq 1$ fm.

The results of our fit are shown in Fig. 3. With the lower limit $\text{Im } a \geq 1$ fm we obtained the total $\chi^2 = 9.6$. The solid lines in Fig. 3 indicate the χ^2+1 , χ^2+2 and χ^2+3 contour lines. Furthermore, the solid circles show different results for $K^- d$ scattering length from the calculations collected in Table 1. It is important to remark that the prediction from Ref. [28] was based on a combined analysis of the experimental results on $K^- d \rightarrow N\Lambda\pi$ and $K^- d \rightarrow N\Sigma\pi$ relative rates and spectra and is quite close to our solution.

Our analysis of the $\bar{K}^0 d$ mass spectra for the $pp \rightarrow d\bar{K}^0 K^+$ reaction allows one to accept

some predictions [28,29,27] for the K^-d scattering length within the range $\text{Im } a \leq 1.3$ fm and $|\text{Re } a| \leq -1.3$ fm. The limit for the imaginary part of the K^-d scattering length is also strongly supported by the data on the total K^-d cross section shown in Fig. 2. Note that the model results listed in Table 1 have been calculated with different input parameters for the elementary K^-p and K^-n scattering lengths, also given in Table 1. The different input as an elementary K^-p and K^-n scattering lengths largely explains the variations in the final results for the K^-d scattering length.

As a next step the elementary K^-p and K^-n scattering lengths might be extracted from our results obtained from the $pp \rightarrow d\bar{K}^0 K^+$ data applying established few-body techniques. In addition the possible interplay of the $\bar{K}K$ interaction and the $\bar{K}d$ interaction, also the influence of a non-vanishing $\bar{K}d$ effective range should be studied.

Acknowledgements

L.A.K. is grateful to the Institut für Kernphysik (Theory) at the Forschungszentrum Jülich for providing hospitality during the course of carrying out this work. This work is partially supported by the Russian Fund for Basic Research (grants 02-02-1673 and 03-02-04025).

REFERENCES

1. A.D. Martin, Nucl.Phys. B179 (1981) 33.
2. T.M. Ito et al., Phys. Rev. C 58 (1998) 2366.
3. C. Guaraldo et al., Eur. Phys. J. A19 (2004) 185.
4. R. H. Dalitz, T. C. Wong, and G. Rajasekaran, Phys. Rev. 153 (1967) 1617.
5. P. B. Siegel and W. Weise, Phys. Rev. C 38 (1988) 2221.
6. M. Lutz, Phys. Lett. B 426 (1998) 12; nucl-th/9709073.
7. A. Ramos et al., Nucl. Phys. A691 (2001) 258c; nucl-th/0101031.
8. H. Heiselberg, M. Hjorts-Jensen, Phys. Rep. 328 (2000) 237.
9. A. Cieply, E. Fridman, A. Gal, J. Mares, Nucl. Phys. A696 (2001) 173.
10. U.-G. Meißner, Rep. Prog. Phys. 56 (1993) 903.
11. G. Ecker, Prog. Part. Nucl. Phys. 35 (1995) 1.
12. A. Pich, Rep. Prog. Phys. 58 (1995) 563.
13. V. Bernard, N. Kaiser and U.-G. Meißner, Int. J. Mod. Phys. E4 (1995) 193.
14. T. Waas, N. Kaiser, and W. Weise, Phys. Lett. B 365 (1966) 12 (1996); Phys. Lett. B 379 (1996) 34; W. Weise, Nucl. Phys. A610 (1996) 35.
15. E. Oset, A. Ramos, Nucl. Phys. A 635 (1998) 99.
16. J.A. Oller and U.-G. Meißner, Phys. Lett B 500 (2001) 263; hep-ph/0011146.
17. D. Jido, J. A. Oller, E. Oset, A. Ramos and U.-G. Meißner, Nucl. Phys. A 725 (2003) 181; nucl-th/0303062.
18. U.-G. Meißner, U. Raha and A. Rusetsky, hep-ph/0402261, Eur. Phys. J. C (2004) in press.
19. U.-G. Meißner and J.A. Oller, Nucl. Phys. A 673 (2000) 311; nucl-th/9912026.
20. J. Marton et al., Int. Conf. QNP2004, Bloomington, 2004.
21. V. Kleber et al., Phys. Rev. Lett. 91 (2003) 172304; nucl-ex/0304020.
22. V.Yu. Grishina, L.A. Kondratyuk, E. L. Bratkovskaya, M. Büscher and W. Cassing, Eur. Phys. J. A 9 (2000) 277; nucl-th/0007074.
23. E. Oset, J.A. Oller and U.-G. Meißner, Eur. Phys. J. A 12 (2001) 435; nucl-th/0109050.
24. V.Yu. Grishina, L.A. Kondratyuk, M. Büscher, W. Cassing, and H. Ströher, Phys. Lett. B 521 (2001) 217; nucl-th/0103081.
25. A. E. Kudryavtsev, V. E. Tarasov, J. Haidenbauer, C. Hanhart, and J. Speth, Phys. Rev. C 66 (2002) 015207; nucl-th/0203034.
26. C. Hanhart, Phys. Rept. 397 (2004) 155; hep-ph/0311341.
27. V.Yu. Grishina, L.A. Kondratyuk, M. Büscher and W. Cassing Eur. Phys. J. (in print); nucl-th/0402093.
28. M. Torres, R.H. Dalitz and A. Deloff, Phys. Lett. B 174 (1986) 213.
29. A. Deloff, Phys. Rev. C 61 (2000) 024004.
30. S. S. Kamalov, E. Oset and A. Ramos, Nucl. Phys. A 690 (2001) 494; nucl-th/0010054.

31. A. Bahaoui, C. Fayard, T. Mizutani and B. Saghai, Phys. Rev. C 66,(2002) 057001; Phys. Rev. C 68 (2003) 064001; nucl-th/0307067.
32. K. M. Watson, Phys. Rev. 88 (1952) 1163.
33. A. B. Migdal, JETP 1 (1955) 2.
34. M. L. Goldberger and K. M. Watson, Collision Theory, John Wiley and Sons, Inc., New York, London, Sidney (1964), p.540.